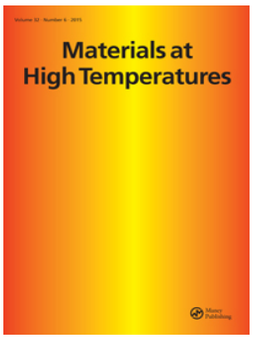

Materials at High Temperatures

ISSN: 0960-3409 (Print) 1878-6413 (Online) Journal homepage: www.tandfonline.com/journals/ymht20

# Experimental and simulation studies on thixoforming of AA 2017 alloy

C. H. Shashikanth & M. J. Davidson

**To cite this article:** C. H. Shashikanth & M. J. Davidson (2015) Experimental and simulation studies on thixoforming of AA 2017 alloy, Materials at High Temperatures, 32:6, 541-550, DOI: 10.1179/1878641314Y.0000000043

**To link to this article:** https://doi.org/10.1179/1878641314Y.0000000043

# Experimental and simulation studies on thixoforming of AA 2017 alloy

**C. H. Shashikanth*[1] and M. J. Davidson[2]**

Thixoforming is one of the near net shaped manufacturing processes which in the product will be formed between the solidus and the liquidus temperatures of the alloy. In the present work, a finite element based simulation study has been performed to simulate the thixoextrusion of AA 2017 alloy in the semisolid range. The alloy has been heated between 570 and 610°C and it was extruded in a die having die cone angles of 30, 45 and 60°. Simulation studies have been performed by using the constitutive relation that was developed by performing disc compression tests at different temperatures and strain rates. A good agreement was found between the experimental and the simulation results.

**Keywords:** Thixoforming, Solidus, Liquidus, Thixoextrusion, Simulation

## Introduction

Owing to their high specific strength and lightweight structure, the age hardenable 2XXX aluminium alloys are widely used in the aircraft structures, as automobiles bodies and other structural applications.[1–3] The material strength of the alloy can be increased by increasing the amount of alloying elements such as Si, Mg, Fe, Mn and Cu.[4] Owing to presence of copper, theses alloys are hard to form at room temperatures. However, the formability of theses alloys can be improved by forming these alloys at elevated temperatures. Owing to dynamic recovery, these alloys provide lower flow stress and higher ductility at elevated temperatures. Products made by casting route lack the desired mechanical strength due to defects such as porosity and cracks. Forging processes offers good mechanical strength, but requires higher forming loads to produce precision product and there is a loss in productivity and economic efficiency due to post processing requirements such as machining.[5] The combined benefit of casting and forging can be used to form successful products of AA 2017 alloy if thixoforming is used. Thixoextrusion can also be called as semisolid metal forming process or mushy state forming process. Thixoforming or semisolid metal forming is one of the emerging technology used for manufacturing of near net shape products.[6] In this process, the final shape of the objects is formed at temperatures between the liquidus and solidus temperatures of the alloy. Thixoforming process has various advantages compared to conventional forming process. It requires less forming loads and it increases the die life in die casting operations. Porosity problem will be eliminated because of the forming load.

[1]Department of Mechanical Engineering, NIT Warangal, AP 506104, India
[2]Department of Mechanical Engineering, NIT Warangal, AP 506004, India

*Corresponding author, email shashikanth.chakunta@gmail.com

Thixoforming is one of the active research areas among researchers. Ko *et al.*[7] used FEM to know the material flow and to simulate the problems in the forming of A356 in mushy state condition. Kumar *et al.*[8] studied the flow response and structural evolution under shear deformation by using a new constitutive relation. The theoretical and experimental data of the isothermal mechanical behaviour of alloys in the mushy state was compared by Nguyen *et al.*.[9] Gunasekera[10] formulated a constitutive equation for mushy state materials using the geometrical shape of the solid particle and the liquid. Numerical analysis of the upsetting process was performed by Toyoshima.[11] Compression behaviour of Sn–15Pb alloy in the semisolid state and the effect of strain rate was studied by Suery *et al.* and Toyosima *et al.*[11,12] Kenny *et al.*[13] suggested that 60–70% of the solid fraction is required to obtain the best quality product. Microstructure and liquid flow state of Al–Cu alloy in the semisolid forming was given by Yoshida *et al.*[14]

The aim of the present study is to formulate a finite element based simulation model capable of simulating the thixoextrusion process while extruding AA 2017 alloy. An Arrhenius type constitutive relation involving the solid fractions and the strain rate has been developed. The developed relation has been used to simulate the thixoforming process in DEFORM 2D, an FEA based simulation software.

## Constitutive relation for thixoforming

A series of mushy state compression tests have been conducted in the temperature ranging from 570 to 610°C and at different strain rates, namely, 0·16, 0·18 and 0·2. An Arrhenius type relation of the form $\dot{\varepsilon} = A[\sinh(\alpha\sigma)]^n \exp[-Q/RT]$ has been developed[15] and the detailed procedure followed in developing the constitutive relation has been reported in an earlier work by the authors[16] The material constants such as $A$, $\alpha$, $\beta$ and $n$, where '$\alpha$' is the stress multiplier, '$n$' is the


Received 8 August 2014; accepted 1 January 2015
DOI 10.1179/1878641314Y.0000000043

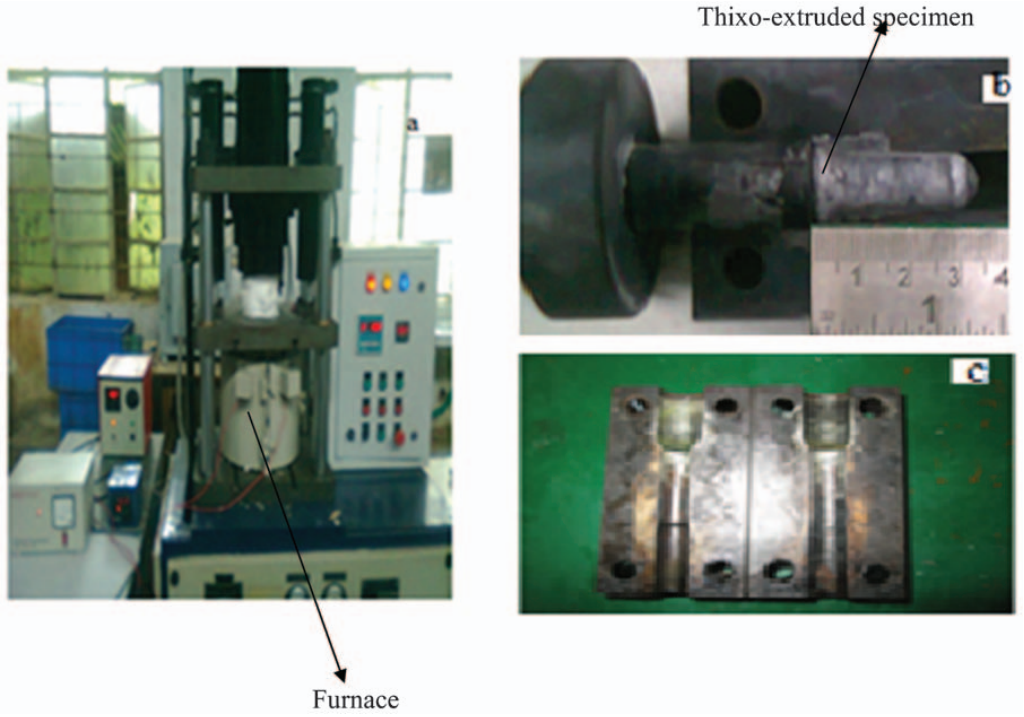


**1 Hydraulic press with furnace attachment**

stress exponent, and '$A$' a dh 'β' are the material constants, have been evaluated by performing disc compression tests at the above temperatures and strain rates. The deformation activation energy '$Q$' which indicates the degree of difficulty during plastic deformation is also calculated. The Zener–Hollomon parameter ($Z$ value) which describes the effect of strain rate and temperature ($T$) on stress and microstructure during hot deformation of metallic materials has been calculated as well.

The deformation load, the initial height of the specimens ($h_i$) and the height of the specimens after compression ($h_f$), the top ($D_{top}$), and bottom ($D_{bot}$) contact diameters and the bulge diameters ($D_b$) were measured after each stage of compressive testing. The load stroke data obtained from the experiments were converted into true stress and true strains. The constitutive relation thus developed is given by

$$\dot{\varepsilon} = A378333{\cdot}2[\sinh(0{\cdot}017\sigma)]^{0{\cdot}614}\exp(-103{\cdot}38/RT) \quad (1)$$

## Differential scanning calorimetric analysis

To perform mushy state compression tests at different temperatures, it is required to know the solidus and liquidus temperatures of an alloy. To know these

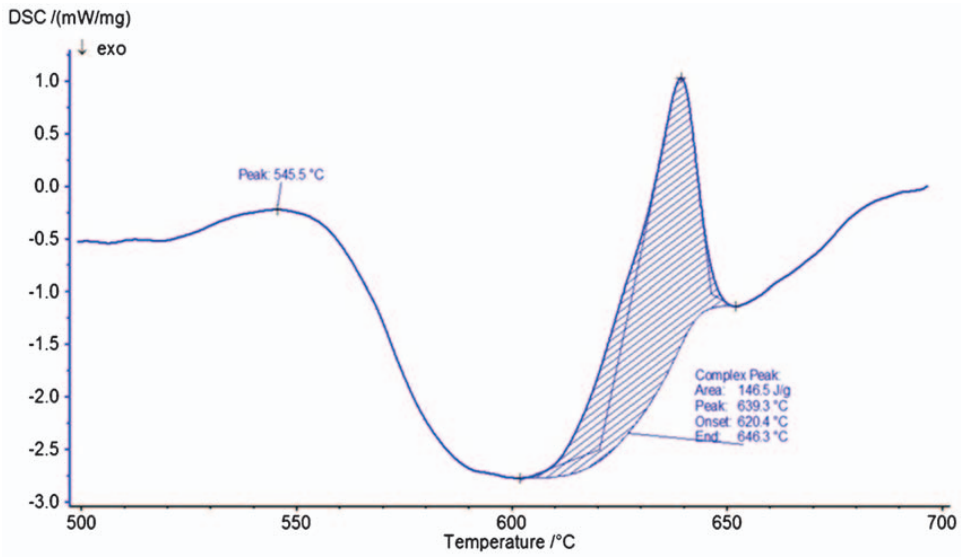


**2 DSC curve of semisolid alloy AA 2017**

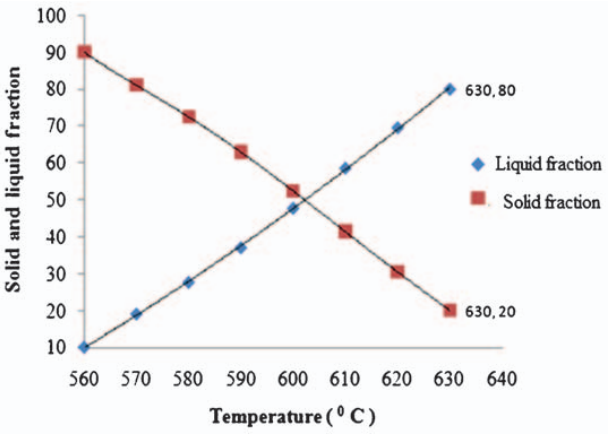


**3 Relationship between the temperature and percentage of solid fraction**

values, differential scanning calorimetric analysis (DSC) of aluminium AA 2017 alloy billet was performed on a NETZSCHSTA 449F integrated thermal analyser. The DSC curve is shown in Fig. 2. The solidus and liquidus temperatures of aluminium AA 2017 alloy were found to be 545 and 646°C respectively. The difference between the liquidus and solidus temperatures is 100°C. The deformation behaviour of material in the mushy state is different from the deformation behaviour at hot compression test. The deformation behaviour of metal in mushy state is influenced by the deformation temperature and the percentage of solid fraction.[17] The relation between the solid fraction and temperature is shown in the Fig. 3. The percentage of solid fraction within the solidification range of an alloy at

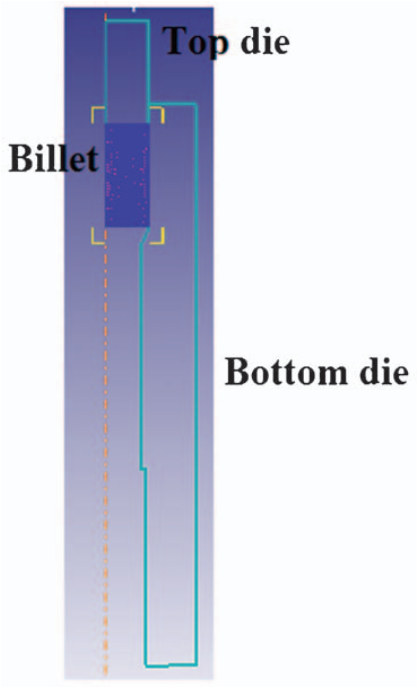


**4 Finite element simulation model**

any given temperature was determined by using Scheil equation (2).[18]

$$f_s = 1-(T_s - T/T_s - T_l)^{(1/1-k)} \quad (2)$$

where $k$ is the partition coefficient, $T_s$ is the solidus temperature and $T_l$ is liquidus temperature.

It was assumed that the liquid is completely homogenised with no diffusion in the solid.[19] The solid fraction of AA 2017 alloy at the temperatures 570, 590

**Table 1 Simulation combinations of thixoextrusion process parameters**

| Simulation no. | Temperature/°C | Strain rate/s$^{-1}$ | Approach angle/° | % reduction in area (RA) |
|---|---|---|---|---|
| 1 | 570 | 0·16 | 30 | 35 |
| 2 | 570 | 0·18 | 45 | 55 |
| 3 | 570 | 0·20 | 60 | 75 |
| 4 | 590 | 0·16 | 45 | 75 |
| 5 | 590 | 0·18 | 60 | 35 |
| 6 | 590 | 0·20 | 30 | 55 |
| 7 | 610 | 0·16 | 60 | 55 |
| 8 | 610 | 0·18 | 30 | 75 |
| 9 | 610 | 0·20 | 45 | 35 |

**Table 2 simulation and experimental results**

| Simulation no. | Temperature/°C | Strain rate/s$^{-1}$ | Approach angle/° | % reduction area (RA) | Simulation load/kN | Experimental load/kN | % loss of volume in experiments | % loss of volume in simulation |
|---|---|---|---|---|---|---|---|---|
| 1 | 570 | 0·16 | 30 | 35 | 17 | 19 | 6 | 3 |
| 2 | 570 | 0·18 | 45 | 55 | 35 | 31 | 11 | 9 |
| 3 | 570 | 0·2 | 60 | 75 | 41 | 47 | 13 | 22 |
| 4 | 590 | 0·16 | 45 | 75 | 49 | 39 | 10 | 28 |
| 5 | 590 | 0·18 | 60 | 35 | 18 | 14 | 15 | 31 |
| 6 | 590 | 0·2 | 30 | 55 | 20 | 27 | 14 | 36 |
| 7 | 610 | 0·16 | 60 | 55 | 23 | 24 | 20 | 49 |
| 8 | 610 | 0·18 | 30 | 75 | 32 | 30 | 28 | 58 |
| 9 | 610 | 0·2 | 45 | 35 | 22 | 19 | 17 | 50 |

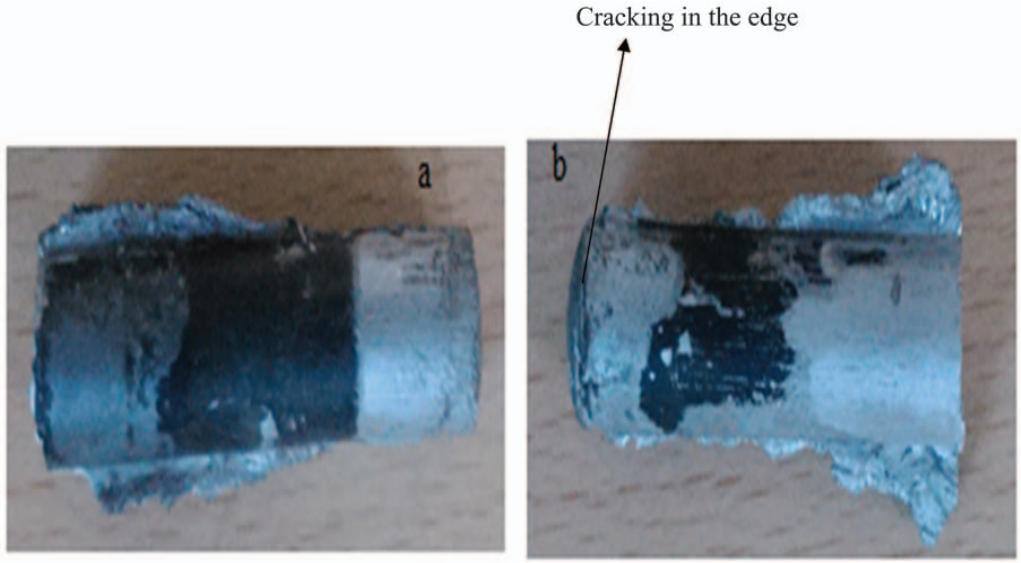


**5 Thixoextruded specimen at *a* 590°C and *b* 610°C**

and 610°C were found to be 0·9, 0·7 and 0·5 respectively from the Scheil equation.

## Finite element analysis of thixoextrusion

During the mushy state forming experiments, the liquid segregation and crack occurs at the free surface of the alloy. These are the two main problems that occur in the mushy state forming. To overcome these problems, different extrusion process parameters are required to control the process optimally. To arrive at the optimum process parameters range for defect free product, finite element based simulations for semisolid extrusion of AA 2017 aluminium alloy has been conducted. The process parameters which are used in this study are as follows.

(i) die temperature (570, 590 and 610°C)
(ii) approach angle of die (30, 45 and 60°)
(iii) reduction area (35, 55 and 75%)
(iv) strain rate (0·16, 0·18 and 0·2).

## Finite element modelling

The finite element based simulation software DEFORM 2D, has been used for the simulation of thixoextrusion process of AA 2017 aluminium alloy billets. Specimens of diameter 15 mm and height 15 mm were used for the simulation study as shown in Fig. 6. The bottom die was fixed. Axisymmetric analysis was performed because the shape of the specimen is axisymmtric. A friction coefficient value of $m=0{\cdot}4$ was assumed between the top die and workpiece interface. The initial solid fraction was assumed as homogeneous. The material constants such as $n$, $\alpha$, $\beta$, $m$ and '$A$' of AA 2017 aluminium alloy evaluated from the mushy state compression tests were used as input variables in the constitutive relation. The constitutive equation (1) developed has been given as input for relating the stresses and strains at various temperatures and strain rates.

## Results and discussion

To analyse the effect of each process parameter on the quality of extrusion product and on the extrusion load, nine different combinations of process parameters were chosen which are given in Table 1. Experimental and finite element simulation studies were performed for all the nine combinations and the results are tabulated in Table 2.

### Effect of solid fraction

Owing to the presence of copper, the extrudability of AA 2017 alloys is difficult and the alloys need high extrusion pressures. However, the alloy is extrudable at semisolid state due to the presence of globular grains at elevated temperatures. Thus, the solid fraction of the alloy is an important process condition for obtaining good products. However, the mechanical and metallurgical properties of the alloy depend on the amount of solid and liquid fractions of the alloy during the extrusion cycle. A mix of solid and liquid particles makes the solid particle to glide through the liquid matrix and makes it easy to form. However, too much liquid fraction at the end of the extrusion cycle results in cracking of the workpiece at the edge. It is preferable to have the workpiece with more liquid fraction in the initial stage of extrusion and more solid at the end of the extrusion cycle. To analyse the quality of product that can be achieved at different liquid and solid fractions, extensive finite element

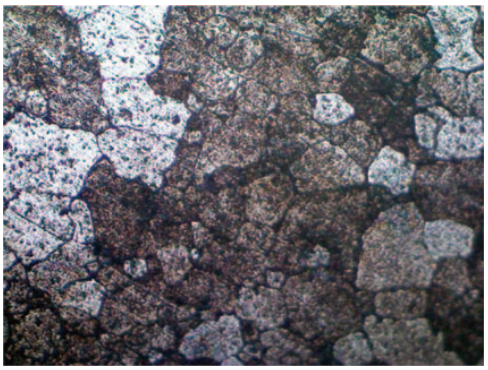

**6 Microstructure of thixoextruded sample extruded at 610°C shows globular grains**

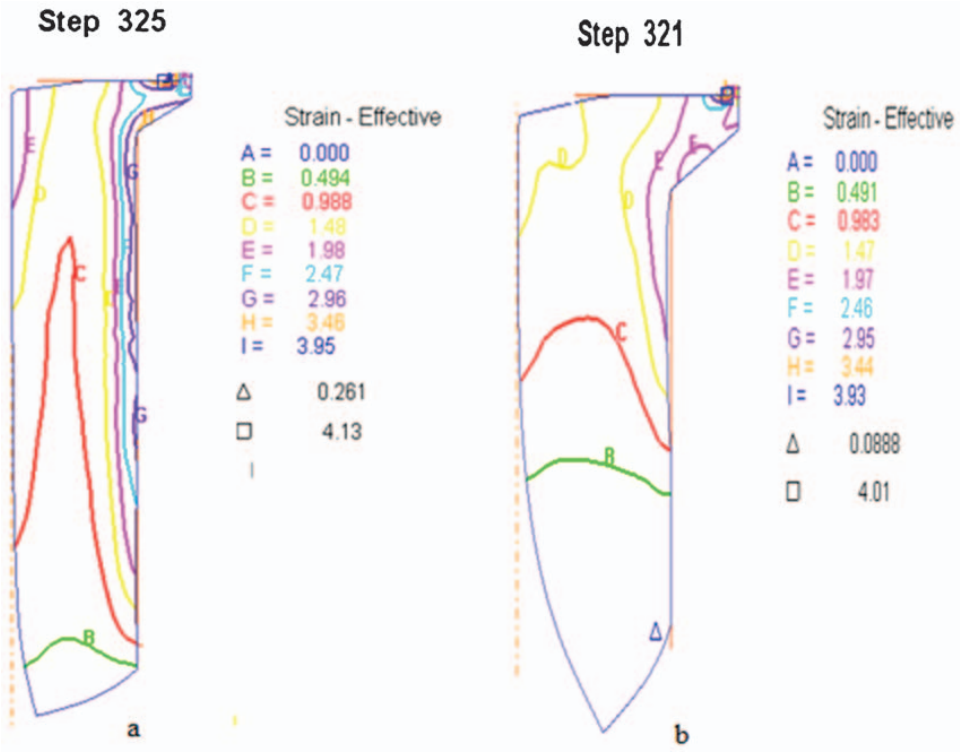


**7 Distribution of effective strain at different solid fractions corresponding to temperatures *a* 570°C and *b* 610°C for die angle of 60° and strain rate of 0·16 $s^{-1}$**

studies have been made with different solid and liquid fractions. The results have been verified with experimental verifications as well. Figure 5 shows the edge of the rod extruded at very high solid and liquid fractions. The microstructure of the alloy extruded at high liquid fraction shows globular grains as seen in Fig. 6.

Figure 7 above shows the distribution of strain at 610 and 570°C. The distribution of strain is found to be uniform at a temperature of 610°C due to the presence of more liquid fraction. The effective stress at 570°C (high solid fraction) was found to be 225 MPa and at low solid fraction (610°C) it was 152 MPa. This lower stress distribution is attributed

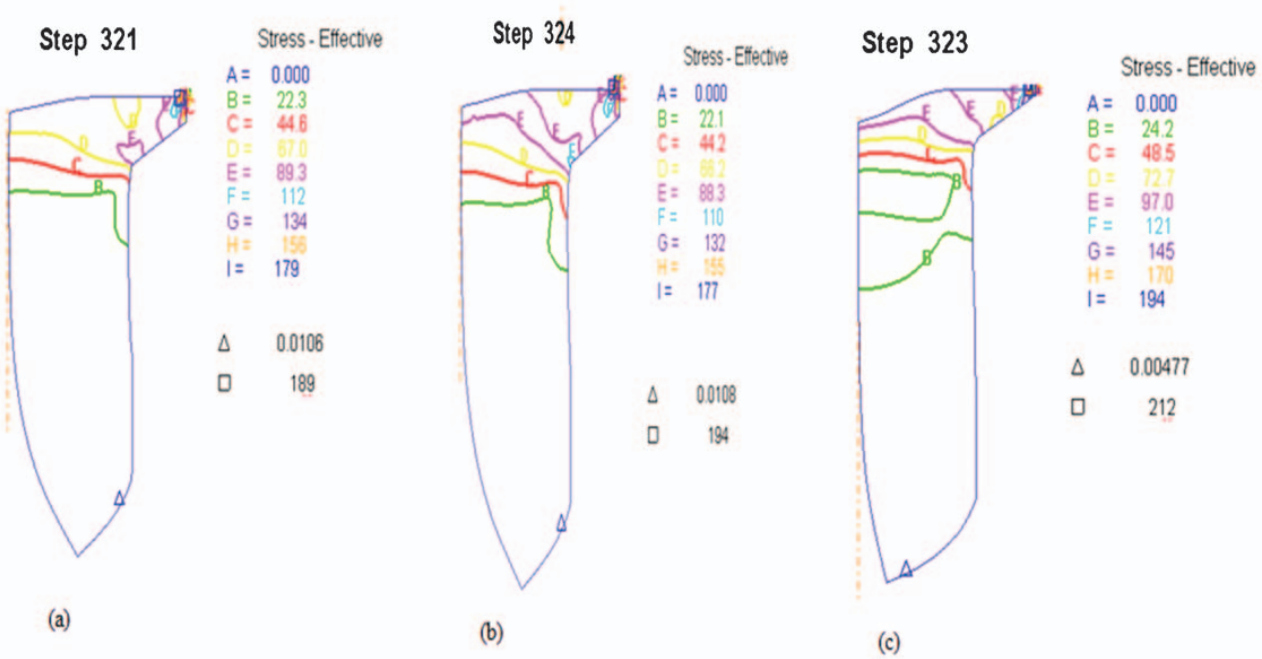


*a* 0·16 $s^{-1}$; *b* 0·18 $s^{-1}$; *c* 0·2 $s^{-1}$

**8 Distribution of effective stress at 610°C, die angle of 60° and strain rate of**

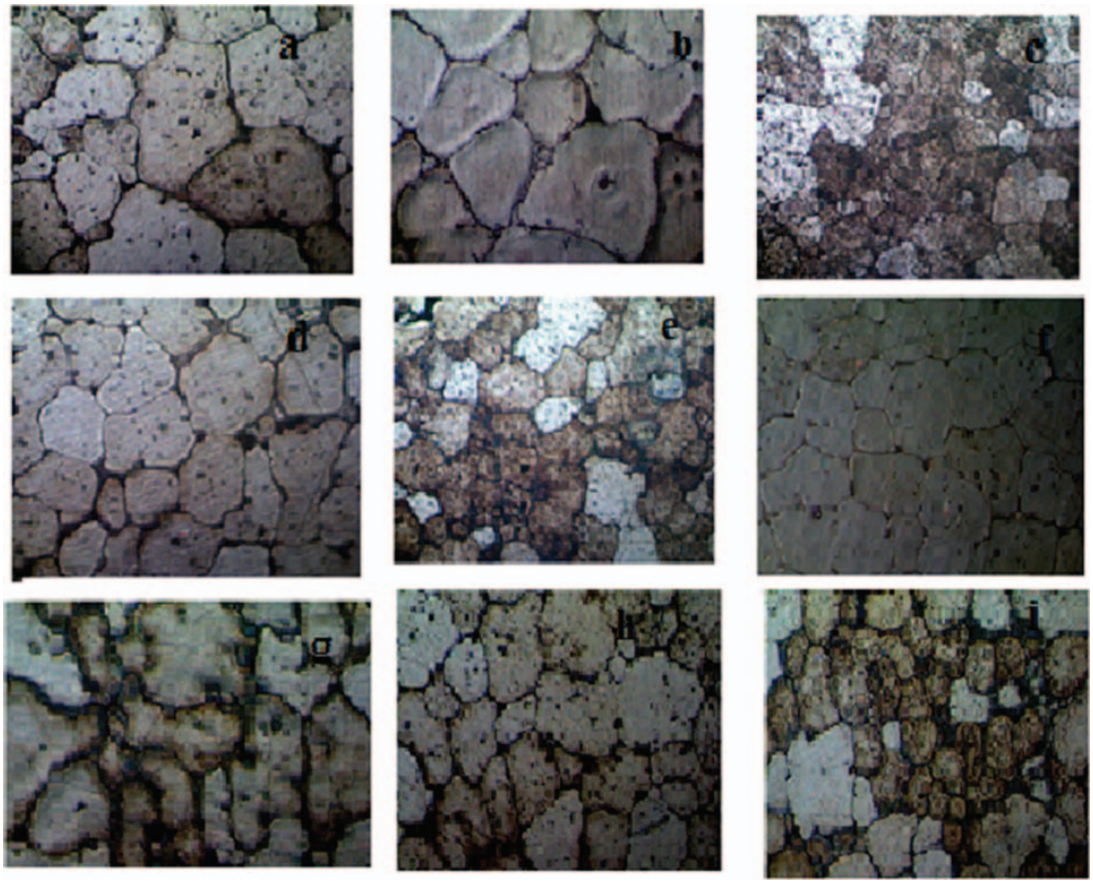


*a* 570°C, 0·16 $s^{-1}$; *b* 590°C, 0·16 $s^{-1}$; *c* 610°C, 0·16 $s^{-1}$; *d* 570°C, 0·18 $s^{-1}$; *e* 590°C, 0·18 $s^{-1}$; *f* 610°C, 0·18 $s^{-1}$; *g* 570°C, 0·2 $s^{-1}$; *h* 590°C, 0·2 $s^{-1}$; *i* 610°C, 0·2 $s^{-1}$

**9 Microstructures of thixoextruded samples at different temperatures and different strain rates**

to the presence of more liquid particles embedded between the solid particles at high temperature, resulting in the solid particles gliding across the liquid medium, resulting in a flow containing liquid flow and solid particles gliding resulting in less stress.

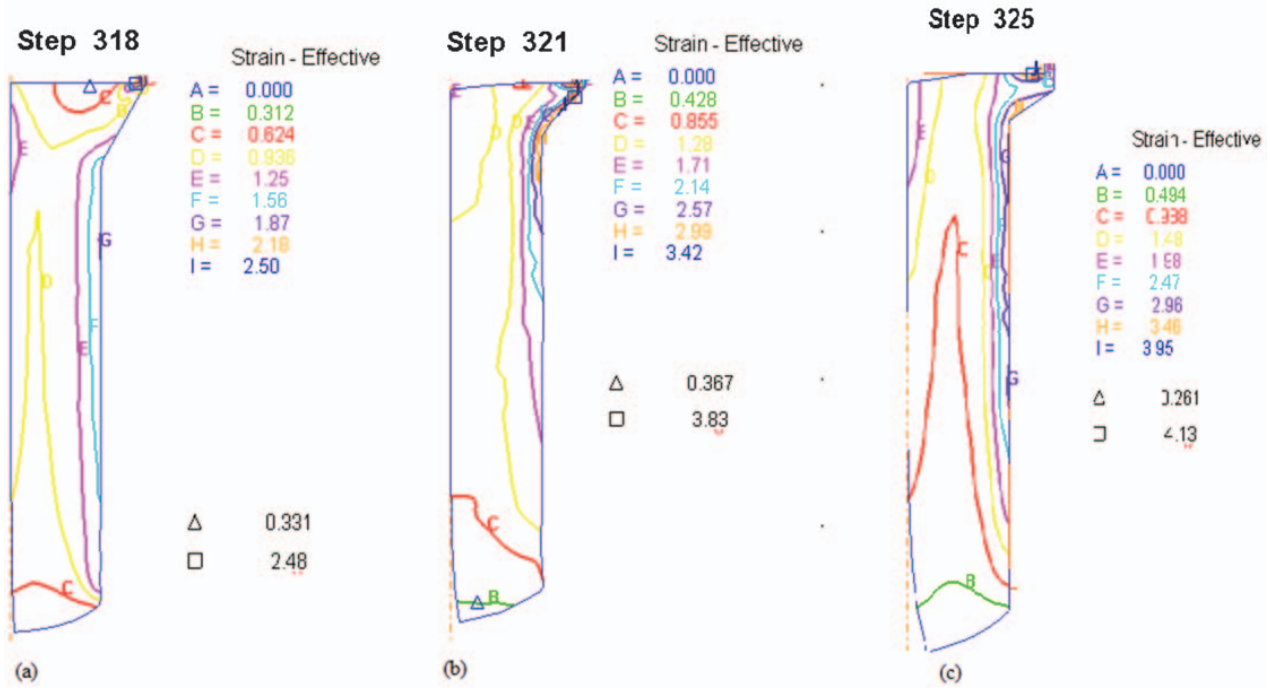


**10 Distribution of effective strain at 570°C and strain rate of 0·16 $s^{-1}$ for approach angles of *a* 30°, *b* 45° and *c* 60°**

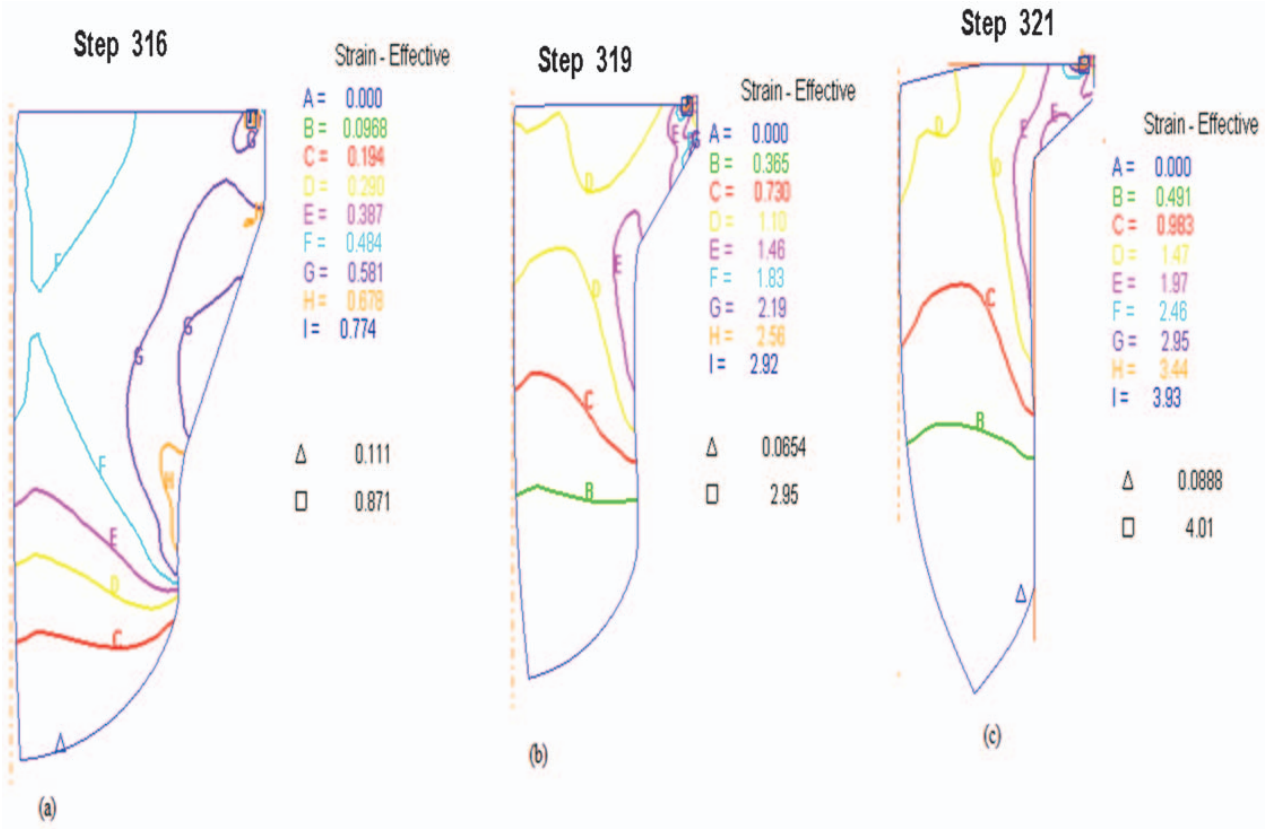


**11 Distribution of effective strain at 610°C and strain rate of 0·16 for approach angles of *a* 30°, *b* 45° and *c* 60°**

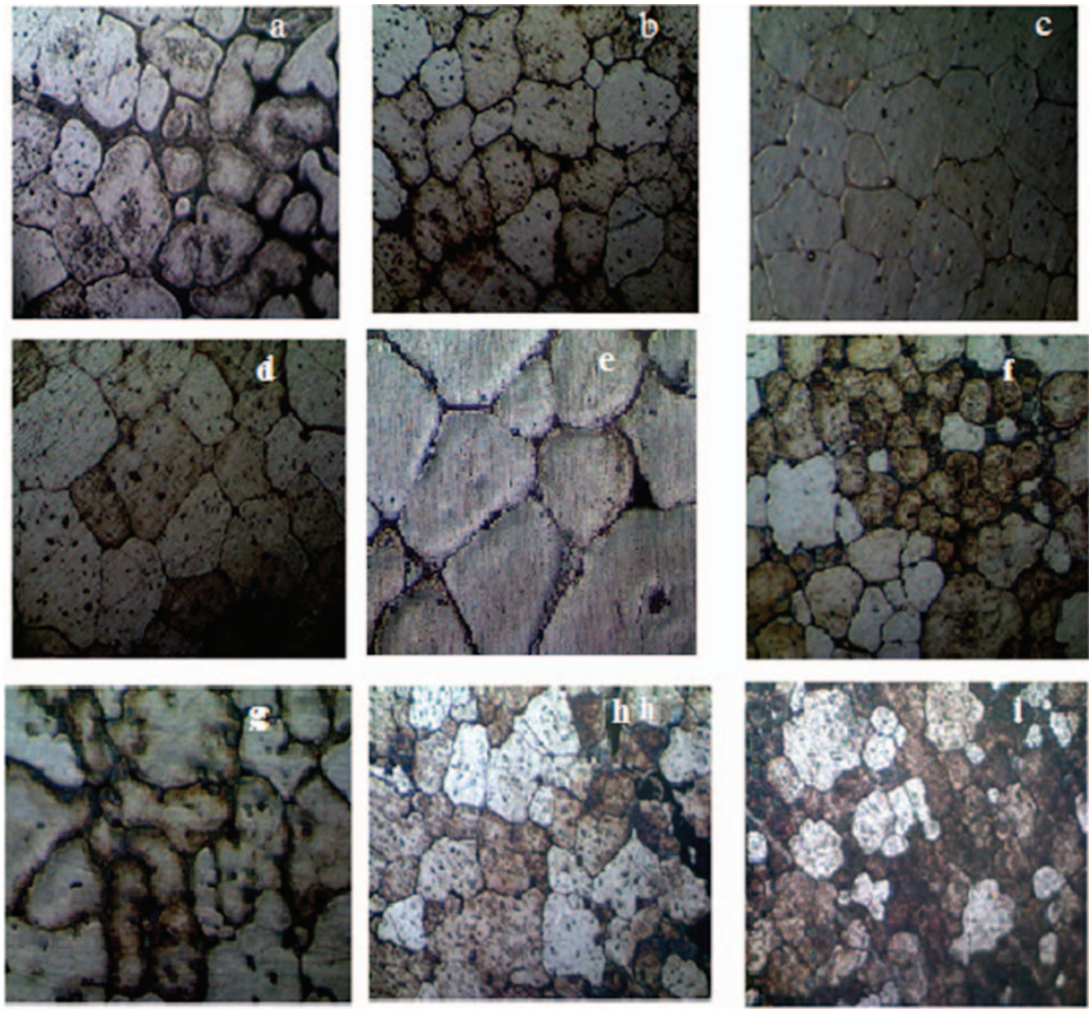


*a* 570°C, 30°; *b* 590°C, 30°; *c* 610°C, 30°; *d* 570°C, 45°; *e* 590°C 45°; *f* 610°C, 45°; *g* 570°C, 60°; *h* 590°C, 60°; *i* 610°C, 60°

**12 Microstructures at different temperatures and different approach angles**

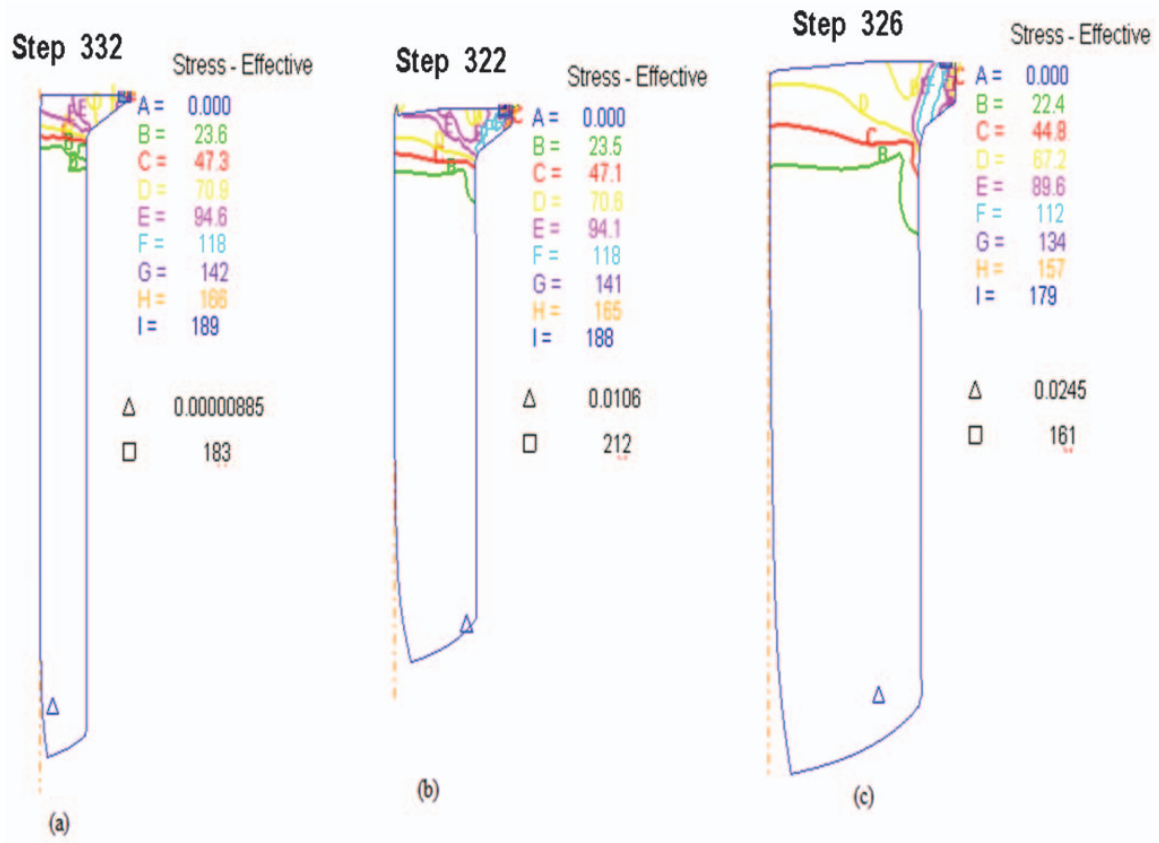


*a* 75%; *b* 55%; *c* 35%

**13 Distribution of effective stress at 570°C, die angle of 60° and strain rate of 0·16 $s^{-1}$**

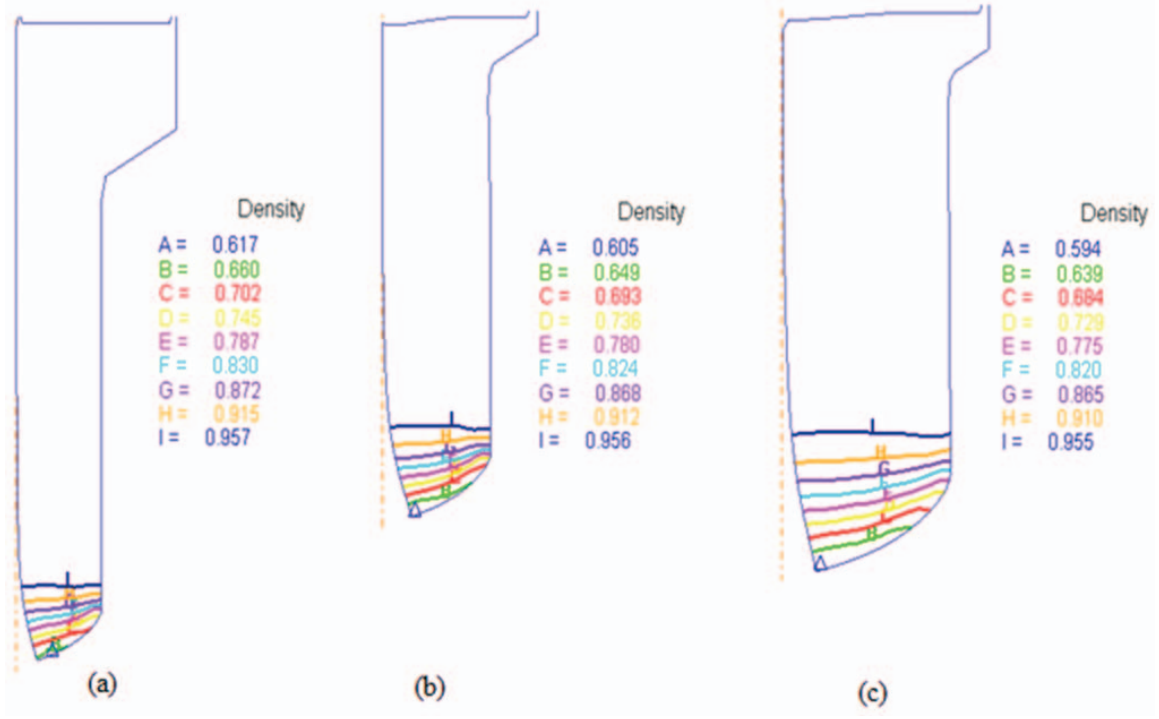


*a* 75%; *b* 55%; *c* 35%

**14 Density at 570°C, die angle of 60° and strain rate of 0·16 $s^{-1}$**

15 Thixoextruded specimen cracked due to fluid segregation

## Effect of strain rate

The strain rate with which the metal is extruded across the die is one of the most important factors that contribute to the success of the product. In the present study, the thixoextrusion study was performed with different strain rates namely, 0·16, 0·18 and 0·20. Figure 8 below shows the effect of strain rate on the effective stress. The effective stress is found to increase with increase in the strain rate. The progression of the top die across the bottom die created primarily two zones of deformation namely dead zone and shear zone. The shear zone was found along the wall of the extrusion die. With increase in strain rate, the shear zone domain was found to increase and hence, the effective strain increased as the strain rate was increased.

Figure 9 shows the microstructures of the alloy extruded at different strain rates ranging from 0·16 to 0·2 for different solid and liquid fractions. The microstructures revels that the in homogeneity of the deformation increases with increase in strain rate at high solid fraction. At high liquid fraction at 610°C the in homogeneity increases with low strain rate. Irrespective of the strain rate, the samples deformed at 590°C were more homogeneous.

## Effect of approach angle

The approach angle of the die facilitates the heated metal to move along the die wall. The variation in the approach die angle creates different frictional conditions on the interface of the wall and the metal. The effective strain is found to be less for the metal extruded with a die with 30° approach angle and it is more for the die with 60° approach angle. A low effective strain implies that the metal being pressed is stronger than the alloy which has undergone higher strain. This implies that a narrower die is required to produce a stronger alloy. Thus, along with higher solid fraction a narrower die produces alloy with higher strength. The variation of effective strain with the die approach angle is shown in Figs. 10 and 11.

Comparing Figs. 10 and 11, it is observed that, the distribution of strain is uniform at higher liquid fraction and within the temperature ranges; the strain distribution is uniform on the samples extruded with higher approach angle.

Figure 12 shows the microstructures of the samples drawn at different temperatures and approach angles. It is evident from Fig. 12a, *d* and *g* that the in homogeneity

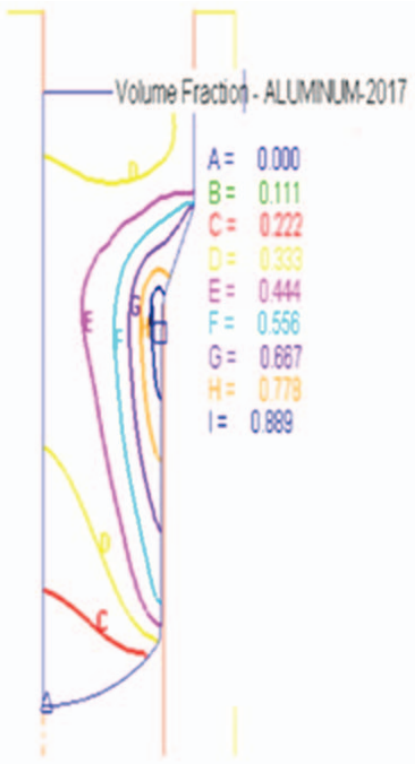


16 Distribution of volume fraction on thixoextruded sample

increases as the approach angle is increased. As the temperature is increased to 610°C, even for high approach angle a globular microstructure was found. However at this temperature more volume loss was experienced due to the fluidity of the sample. Irrespective of the approach angles, the sample deformed at 590°C, Fig. 12*b*, *e* and *h* resulted in a more homogeneous deformation.

## Effect of percentage reduction in area

The percentage reduction in area of the extrudate is proportional to the die diameter. The narrower the die, the stronger will be the alloy at the end of the extrusion stroke. Figure 13 shows the plot of the effective stress for different percentage reductions. The effective stress is found to be more for the alloy produced in a die with narrow approach angle Fig. 13*a*.

It is observed from Fig. 14 that with increase in percentage reduction, the solid fraction increases. This shows that the amount of deformation is closely related to the densification of the solid phase. The densifications attained by the samples were measured by noting down their densities after the forming cycle. The large force with which the semisolid alloy is squeezed through the die has made the alloy to densify in the narrow exit portion of the extrusion die. This is the reason why the solid fraction increases with increase in percentage reduction. As it is evident from Fig 14, the solid fraction of the alloy increases as the semisolid slurry enters the converged portion of the die. Moreover, from Table 2, it is evident that the approach angle and the percentage reduction in area of the exit portion of the die plays a vital role in the deformation behaviour of the alloy. A narrow approach angle of die and increased percentage reduction in area increases the solid fraction and the deformation load. This shows that, at the exit portion of the die, due to the above factors, the solid fraction of the

alloy increases and the alloy is extruded nicely. However, when the alloy is extruded out, due to liquid segregation and loss of pressure, small cracks were seen at the end of the workpiece. As the liquid phase flows heavily towards the free surface of die, liquid segregation happens and thus the alloy cracks. A rod that cracked due to fluid segregation is shown in Fig. 15.

### Effect of volume loss

Volume loss during thixoforming is the loss in volume due to the excessive heating of the alloy. The semisolid slurry at the high temperature sticks to the dies, flows freely across the die to a smaller extend and loses its volume. From the simulation and the experiments, it is found that the volume loss is more at high temperatures. It is also observed that, for the same strain rate, the volume loss is more for the experiments performed with a low initial solid fraction. The distribution of volume fraction on a thixoextruded sample is given in Fig. 16.

Thus, it can be concluded that the initial solid fraction is one of the important parameters responsible for volume loss and homogeneous deformation. Also it is observed that homogeneous deformation is obtained when the initial solid fraction is high.

## Conclusions

An experimental and simulation studies have been performed on the thixoextrusion of AA 2017 aluminium alloy. The experiments were conducted at different temperatures from 570 to 610°C, strain rates from 0·16 to 0·20, approach angle of the die from 30 to 60° and percentage reduction in area from 35 to 75%.

The following conclusions have been drawn:

1. The nature of effective strain has similar tendency as that of solid fraction. This shows that the amount of deformation is closely related to the densification of the solid phase.

2. Increasing approach angle of die and percentage reduction of area increases the effective strain and the deformation load. Approach angle and the percentage reduction in area at the exit portion of the die plays a vital role in the deformation behaviour of the alloy.

3. The simulation results and experimental results are close to each other.

## References


1. I. Özbek: 'A study on the re-solution heat treatment of AA 2618 aluminium alloy', *Mater. Charact.*, 2007, **58**, (3), 312–317.
2. C. Y. Xie, R. Schaller and C. Jaquerod: 'High damping capacity after precipitation in some commercial aluminium alloys', *Mater. Sci. Eng. A*, 1998, **A252**, 78–84.
3. Z. Huda, M. Saufi and R. Shaifulazuar: 'Mechanism of grain growth in an aerospace aluminum alloy', *J. Ind. Technol.*, 2006, **15**, 127–136.
4. R. S. Rana, R. Purohit and S. Das: 'Reviews on the influences of alloying elements on the microstructure and mechanical properties of aluminium', *Int. J. Sci. Res. Publ.*, 2012, **2**, 1–7.
5. C. G. Kang, K. D. Jung and H. K. Jung: 'Control of liquid segregation of semi-solid aluminium alloys during intelligent compression test', Proc. 2nd Int. Conf. on 'Intelligent processing and manufacturing of materials', Honolulu, HI, USA, June 1999, IEEE, Vol. 1, 593–599.
6. M. Kiuchi: 'Metal forming in mushy state', in: 'Plasticity and modern metal-forming technology', (ed. T. Z. Blazynski), Chapter 11, 289–313; 1989, New York, Elsevier Applied Science.
7. M. Ko, V. Vazquez, T. Witulski and T. Altan: 'Application of the finite element method to predict material flow and defects in the semi-solid forging of A356 aluminium alloys', *J. Mater. Process. Technol.*, 1996, **59**, 106–112.
8. P. Kumar, C. L. Martin and S. Brown: 'Constitutive modelling and characterization of the flow behaviour of semi-solid metal alloy slurries', *Acta Metall. Mater.*, 1994, **42**, 3595–3614.
9. T. G. Nguyen, D. Favier and M. Suery: 'Theoretical and experimental study of the isothermal mechanical behaviour of alloys in the semi-solid state', *Int. J. Plast.*, 1994, **10**, 663–693.
10. J. S. Gunasekera: 'Development of a constitutive model for mushy materials', Proc. 2nd Int. Conf. on 'Semi-solid processing of alloys and composites', 211–222; 1992, Cambridge, MA, MIT.
11. S. Toyoshima: 'A FEM simulation of densification in forming processes for semi-solid materials', Proc. 3rd Int. Conf. on 'Semi-solid processing of alloys and composites', Tokyo, Japan,1994, 47–62.
12. M. Suery and M. C. Flemings: 'Effect of strain rate on deformation behaviour of semi-solid dendritic alloys', *Metall. Trans.*, 1982, **13**, 1809–1819.
13. M. P. Kenny, J. A. Courtois, R. D. Evans, G. M. Farrior, C. P. Kyonka, A. A. Couch and K. P. Young: 'Semi-solid metal casting and forming', in 'Metals handbook', 9th edn, Vol. 15, 327–338; Materials Park, OH, ASM International.
14. C. Yoshida, M. Moritaka, S. Shinya, S. Yahata, K. Takebayashi and A. Nanba: 'Semi-solid forging of aluminium alloys', Proc. 2nd int. Conf. on 'Processing of semi-solid alloys and composites', 295; 1992, Cambridge, MA, MIT.
15. C. Sellars and W. M. Tegart: 'On the mechanism of hot deformation', *Acta Mater.*, 1966, **14**, 1136–1138.
16. C. H. Shashikanth and M. J. Davidson: 'Simulation studies on deformation behaviour of AA 2017 alloy in the semi-solid state using FEA', *Mater. High Temp.*, 2014, **31**, 3.
17. A. A. Tseng, J. Horsky, M. Raudensky and P. Kotrbacek: 'Deformation behaviour of steel in mushy state', *Mater. Des.*, 2001, **22**, 83–92.
18. K. P. Solek, R. M. Kuziakand and M. Karbowniczek: 'The application of thermodynamic calculations for the semi-solid processing design', *Arch. Metall. Mater.*, 2007, **52**, 1.
19. C. G. Kang, N. H. Kim, B. M. Kim: 'The effect of die shape on the hot extrudability and mechanical properties of 6061 Al/$Al_2O_3$ composites', *J. Mater. Process. Technol.*, 2000, **100**, 53–62.